Clinica Chimica Acta 495 (2019) 656–663

Contents lists available at ScienceDirect

Clinica Chimica Acta

journal homepage: www.elsevier.com/locate/cca

Ectopic expression of factor VIII in MSCs and hepatocytes derived from rDNA targeted hESCs

Qianru Sun, Xionghao Liu, Yong Wu, Wenbin Niu, Panpan Long, Jing Liu, Ming Lei, Youjin Hu, Lingqian Wu, Zhuo Li*, Desheng Liang*

Center for Medical Genetics, School of Life Sciences, Central South University, Changsha, Hunan 410078, China.

ARTICLE INFO

Keywords:
Hemophilia A
Ribosomal DNA
Gene targeting
Human embryonic stem cells
Mesenchymal stem cells
Hepatocytes

ABSTRACT

Hemophilia A is an X-linked recessive bleeding disorder caused by *FVIII* gene deficiency, which may result in spontaneous joint hemorrhages or life-threatening bleeding. Currently, cell-based gene therapy *via ex vivo* transduction of transplantable cells with integrating gene-expressing vectors offers an attractive treatment for HA. In present study, we targeted an expression cassette of B-domain-deleted *FVIII* into the ribosomal DNA (rDNA) locus of human embryonic stem cells (hESCs) by transfection with a nonviral targeting plasmid pHrn. The targeted hESCs clone could be expanded and retained the main pluripotent properties of differentiation into three germ layers both *in vitro* and *in vivo*. Importantly, under defined induction conditions, the targeted hESCs could differentiated into functional mesenchymal stem cells (MSCs) and hepatocytes, as validated by relevant specific cell markers and functional examination. Tumorgenesis assay demonstrated that these cells are relatively safe for future applications. Analysis on gene expression revealed that exogenous *FVIII* mRNA and *FVIII* proteins were both present in differentiated MSCs and hepatocytes. These results indicated that through gene targeting at hESCs rDNA locus a persistent cell source of transplantable genetic-modified cells can be accomplished for HA therapy.

1. Introduction

Hemophilia A (HA) is an X-chromosome-linked recessive bleeding disorder caused by genetic mutation in *FVIII* gene. The clinical symptoms are mainly spontaneous or traumatic hemorrhage, especially in muscle and joint, which can lead to disability and even be life-threatening due to intracranial hemorrhage [1]. Traditional treatment for HA patients is replacement therapy with intravenous infusion of plasma-derived or recombinant FVIII proteins. However, short half-life of FVIII, costly repeated infusions and potential inhibitory antibodies limit its long term application [2].

Since hemophilia A is a monogenic disease and any increase of FVIII levels will be beneficial to patients, the disease is a suitable model for gene therapy. In recent years, although viral vector-based gene therapy for hemophilia A has been conducted in clinical trials [3, 4], its application as a therapy was restricted by possibilities of random insertional mutagenesis, carcinogenesis, and immune responses [5, 6]. In previous studies, we have developed a non-viral targeting vector named pHrn, which is able to mediate exogenous gene integration into the ribosomal DNA (rDNA) locus with high efficiency [7, 8]. This system may profit from multi-copies of rDNA gene and high homologous recombination activity in this area [9, 10]. Furthermore, natural length polymorphism of rDNA area suggests that rDNA locus could serve as a safe harbor for transgene [11]. By utilizing this vector, we have successfully targeted gene addition at the rDNA locus in multiple cell types [7, 8, 12, 13].

Currently, cell-based gene therapy *via ex vivo* transduction of transplantable target cells with integrating gene-expressing vectors offers an attractive treatment for HA. Since the primary site of FVIII synthesis is liver, either hepatocytes or liver sinusoidal endothelial cells as candidate transplanted cells have been used for intervention of HA [2, 14, 15]. However, several studies with transplantation of liver cells in animals failed to detect the FVIII, suggesting the immune suppression or suitable microenvironments may be required [16–19]. Mesenchymal stem cells (MSCs) have been reported to enhance graft facilitation when transplanted with other therapeutic cells by immunosuppressive properties and secretion of bioactive trophic factors [20, 21]. In addition, both hepatocytes and MSCs had been proven to contribute to the functional FVIII pool [22, 23]. Previous studies have demonstrated that injection of *FVIII*-transduced hepatocytes or MSCs increased FVIII in

* Corresponding author at: Center for Medical Genetics, School of Life Sciences, Central South University, 110 Xiangya Road, Changsha, Hunan 410078, China.
E-mail addresses: lizhuo@sklmg.edu.cn (Z. Li), liangdesheng@sklmg.edu.cn (D. Liang).

https://doi.org/10.1016/j.cca.2018.08.007
Received 26 June 2018; Received in revised form 31 July 2018; Accepted 4 August 2018
Available online 07 August 2018
0009-8981/ © 2018 Elsevier B.V. All rights reserved.

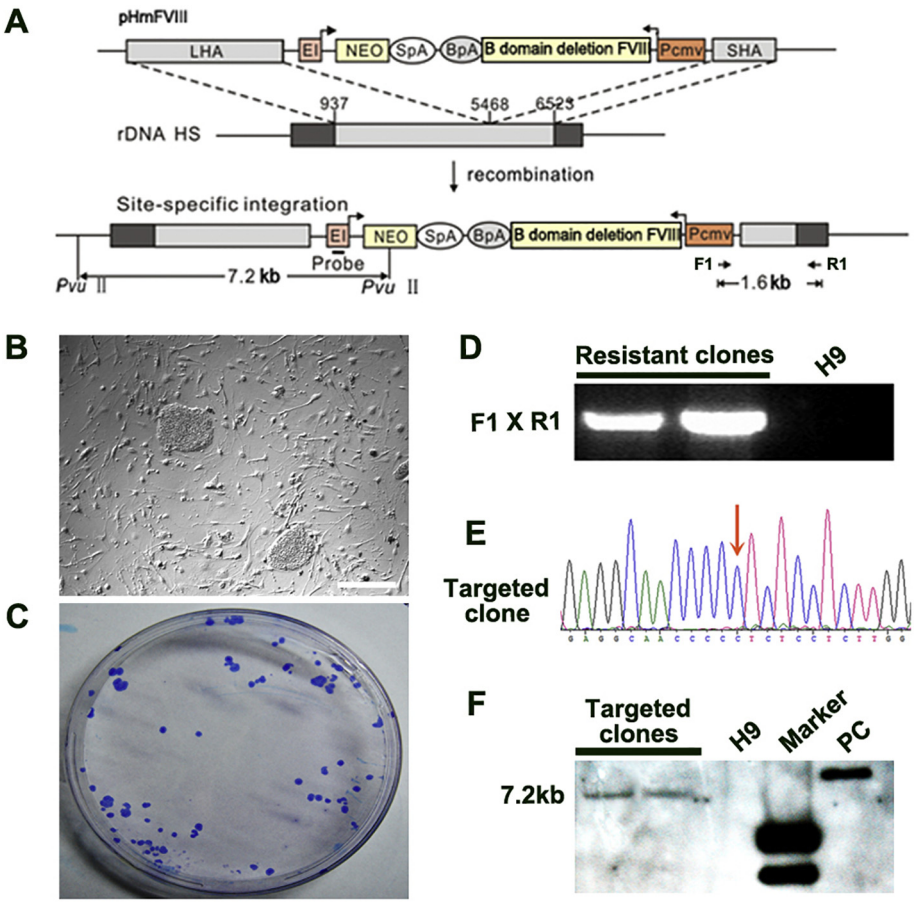

Fig. 1. Site-specific integration at the rDNA locus of hESCs. (A) Schematic of the gene-targeting vector, rDNA unit and targeted allele after HR. The neomycin (Neo) cassette comprises an IRES element, the neomycin gene-coding region, and the SV40 polyA signal (SpA). Neo is transcribed by the promoter of endogenous rRNA genes after HR. The B-domain-deleted *FVIII* gene is driven by the CMV promoter. Integration of NEO to the rDNA unit caused an addition of *Pvu*II site resulting in fragments of 7.2 kb after digestion. LHA and SHA represents long and short homology arm respectively. (B) Morphology of resistant hESCs clones after G418 selection on day 7. Scale bar = 200 μm. (C) After two weeks of drug selection, 50 resistant clones were picked up and the remaining clones were stained with Giemsa. (D) PCR analysis of genomic DNA from resistance clones using primers F1 and R1. PCR products showing a 1.6 kb fragment indicated the occurrence of homologous recombination. (E) DNA sequencing of the PCR product revealed site-specific integration in the rDNA region. Red arrow indicated the junction point between the two homology arms. (F) The PCR-positive clones were confirmed by Southern blotting analysis of the PvuII-digested genomic DNA. Southern blotting displayed a 7.2 kb band for targeted hESCs clones using the designed probe. pHrn vector (10.4 kb) served as a positive control (PC). (For interpretation of the references to colour in this figure legend, the reader is referred to the web version of this article.)

various small and large animal models of HA [15, 24–26]. However, most of somatic cells display a limited proliferation capacity or even lose their cell characteristics during *in vitro* culturing [27, 28]. Therefore, a new strategy to rapidly obtain transplantable cells for use in HA cell therapy is needed.

Human embryonic stem cells (hESCs) and induced pluripotent stem cells (iPSCs) possess potential for self-renewal, proliferation and pluripotency, allowing differentiation into cells of all three germ layers. Both hESCs and iPSCs could differentiate into adequate MSCs and hepatocytes for transplantation use [29–31]. Although iPSCs-derived cells hold an advantage of low immune rejection for personalized transplantation, safety concerns for genomic instability and potential transformation into tumor cells due to the oncogenic properties caused by reprogramming factor (c-MYC) and retroviral or lentiviral vectors becomes more significant [32]. Nonetheless, hESCs-derived retinal pigment epithelium cells have been approved to treat 4 patients with macular degeneration or dystrophy without adverse effect after 1 year of follow-up [33]. Moreover, recent studies have reported that mouse ESCs transfected with human *FVIII* gene could be induced into liver-like embryoid bodies and transplanted into the spleen of SCID mice, resulting hFVIII-antigen production in mouse plasma [34, 35].

In this study, based on hESCs, we sought to investigate an alternative gene therapy strategy that may result in sustained *FVIII* transgene expression. We efficiently and stably targeted a B-domain-deleted *FVIII* expression cassette into the rDNA locus of hESCs using nonviral targeting vector pHrn. Targeted clones retained main characteristics of hESCs and were capable of differentiation into candidate transplantable cells, such as functional MSCs and hepatocytes. Both of the differentiated cells exhibited transcription of exogenous *FVIII* mRNA and increase of *FVIII* secretion. The study may provide a novel stem-cell based strategy for HA therapy and other bleeding disorders.

2. Materials and methods

2.1. hESCs culture and animal use

The human embryonic stem cell line H9 (National Stem Cell Bank) was grown on mitomycin-C treated mouse embryonic fibroblasts (MEF) in DMEM/F12 supplemented with 20% (vol/vol) knockout serum replacement (KSR), 10 ng/ml bFGF, 100 U/ml penicillin, 100 mg/ml streptomycin (P/S), 2 mM L-glutamine, 0.1 mM nonessential amino acids (all from Life Technologies), and 0.1 mM β-mercaptoethanol (β-ME). All studies involving rodent animals followed the guidelines of ARRIVE, the U.K. Animals (Scientific Procedures) Act, EU Directive 2010/63/EU for animal experiments, the National Institutes of Health guide for the care and use of Laboratory animals, and were approved by the Central South University Institutional Animal Care and Use Committee.

2.2. Electroporation of hESCs

The targeting plasmid (pHrn-FVIII) [8] was linearized using *Kpn*I restriction enzyme (NEB). For DNA electroporation, hESCs were collected by accutase (Millipore) and dissociated into single cells by trituration. 2×10^6 cells were electroporated using a BioRad gene pulser (BioRad, 250 V/500 μFd in 500 ml hESCs medium + 300 ml phosphate-buffered saline containing 20 μg of the linearized targeting plasmid). After electroporation, the cells were plated on MEF cells at 0.5×10^6 cells/10 ml. Three days later, G418 (Life Technologies) was added to the culture medium at 25 μg/ml. The concentration of G418 was increased to 50 μg/ml on day 7 posttransfection. Medium was changed every day. Two weeks later, resistant clones were picked and expanded for further experiments.

2.3. PCR and southern blotting detection for gene targeting

Genomic DNA was prepared from individual drug-resistant colonies by a miniprep procedure and used as template for PCR. Primer F1 (5′-AAT GGG CGG GGG TCG TTG GGC GGT CA-3′) was located in CMV promoter (Fig. 1A). Primer R1 (5 -GGC GAT TGA TCG GCA AGC GAC GCT CAG ACA G-3′) was located out of the homologous arm of rDNA locus (Fig. 1A). The putative fragment amplified from site-integration clones is 1.5 kb. The cycling parameters are as follows: 97 °C, 5 min for initial denature; 97 °C, 30 s, 72 °C, 2.5 min, 10 cycles (−0.6 °C/cycle); 97 °C, 30 s, 66 °C, 30 s, 72 °C, 2 min, 25 cycles; 72 °C, 10 min for final extension.

For Southern blotting analysis, genomic DNA (10 μg) was digested with *Pvu* II and separated on a 0.8% agarose gel before being transferred onto a Hybond N+ membrane (Amersham). The hybridization probe was a 330 bp fragment of EMCV-IRES. Using pHrn-FVIII as template, probe was amplified by using the following primer set: forward 5′-CCC GGA AAC CTG GCC CTG TCT T-3'and reverse 5′-TGG GGT ACC TTC TGG GCA TCC TTC-3′. The cycling parameters were as follows: 97 °C, 5 min for initial denature; 97 °C, 30 s, 60 °C, 20 s, 72 °C, 30 s, 32 cycles; 72 °C, 10 min for final extension. The membrane was hybridized overnight at 42 °C to the probe labeled with DIG-dUTP and the signals were detected by AP-conjugated DIG-Antibody (Roche Diagnostics).

2.4. Karyotyping

Cell clumps were treated with 0.08 μg/ml colcemid (Sigma) for 2.5 h. Then the cells were trypsinized, centrifuged and incubated in 0.075 M KCl for 30 min at 37 °C. After fixation with Carnoy fixative, the metaphase chromosome spreads were prepared using air drying method.

2.5. Alkaline phosphatase staining and immunofluorescent staining

Alkaline phosphatase staining for hESCs was performed as described by the manufacturer (Millipore). For immunofluorescence staining, cells were fixed with phosphate-buffered saline (PBS) containing 4% paraformaldehyde for 10 min at room temperature. After washing with PBS, the cells were treated with PBS containing 1% bovine serum albumin, and 0.1% Triton X-100 for 45 min at room temperature. Primary antibodies included anti-SSEA1, anti-SSEA4, anti-TRA-1-60, anti-TRA-1-81 (1:100–1:50, Millipore). Secondary antibodies used were cyanine3 (cy3)-conjugated IgG (1:500. Jackson Immunoresearch). Nucleuses were stained with 1 μg/ml DAPI (Sigma).

2.6. In vitro differentiation

hESCs harvested by trypsinization were transferred to culture dishes in the ES medium without G418. Cell clumps were incubated with 1 mg/ml dispase (Life Technologies) for 10 min at 37 °C, and then washed with DMEM/F12 (Life Technologies). After cultured on Ultra-low attachment plates (Corning) for 7 days in hESC medium with bFGF, embryoid bodies (EBs) were transferred onto gelatin coated coverslips and cultured for another 7 days. Differentiated cells were analyzed by immunofluorescent staining as described above with primary antibodies of anti-AFP (1:100), anti-SMA (1:200), anti-Nestin (1:200) (Millipore), and anti-Tuj1 (1:300) (Sigma).

2.7. Teratoma formation and histological analysis

hESCs cells were suspended at a concentration of 1×10^7 cells/ml in 140 μL DMEM/F12 and 60 μl Matrigel (BD Bioscience). 200 μl of the cell suspension (2×10^6 cells) were injected subcutaneously into the forelimbs of nude mice. Eight weeks after the injection, tumors were surgically dissected from the mice. Samples were weighed, fixed in PBS containing 4% formaldehyde, and embedded in paraffin. Sections were stained with hematoxylin and eosin.

2.8. Differentiation into MSCs and hepatocytes from hESCs

To differentiate hESCs into MSCs, cells were trypsinized and re-suspended in knock-out DMEM medium supplemented with 10% KSR, 1% NEAA, 2 mM L-glutamine, 0.1 mM β-mercaptoethanol, 10 ng/ml bFGF, 20 ng/ml EGF and 20 ng/ml PDGF BB (all from Life Technologies), and the cells were cultured in the 6-well plates. After being passaged 4–5 times with 0.05% Trypsin/EDTA, cells were sent for flow cytometry analysis with a FACSCalibur flow cytometer (BD Biosciences). Differentiation of MSCs into adipocytes, chondrocytes, and osteocytes were performed with GIBCO STEMPRO Differentiation Kit and characterized as previously described [13].

To differentiate hESCs into hepatocytes, embryoid bodies(EB) were generated by dissociating cells with collagenase/dispase on Petri-grade dishes for 48 h in DMEM/F12 supplemented with 10% KSR, 1 mM nonessential amino acids (NEAA), and 1% L-glutamine. For further differentiation, embryoid bodies (EBs) were plated on matrigel™ (BD Biosciences), and maintained for 6 days in DMEM/F12 medium supplemented with 2.5 mmol/L sodium butyrate (Sigma-Aldrich), 10 ng/ml bFGF (Life Technologies), and 100 ng/ml Activin A (PeproTech). 6 days after induction, the cells were grown in differentiation medium supplemented with 20 ng/ml HGF, 10 ng/ml FGF4,10 ng/ml BMP4, and 10 ng/ml OSM (all from R&D Systems) for an additional 6 days. For the final 3 days of culture, cells were treated with 0.1 μmol/L Dexamethasone (Sigma-Aldrich) and 10 ng/ml OSM. Differentiated cells were characterized by RT-PCR for hepatocyte specific markers (AFP, ALB, AAT, CYP7A1) and immunofluorescent staining as described above with primary antibodies of anti-AFP (1:100), anti-ALB (1:200) and anti-AAT (1:200) (all from Santa Cruz).

2.9. Periodic Acid-Schiff staining and indocyanine green uptake assay

Periodic Acid-Schiff (PAS) staining kit (Sigma-Aldrich) was used to determine glycogen storage as described in the manufacture's protocol. Cellular uptake and release of indocyanine green (ICG) (Sigma-Aldrich) assay was applied to verify the hepatocytes function. Briefly, cells were incubated in medium with 1 mg/ml diluted ICG for 60 min at 37 °C. After washing with PBS, cellular uptake of ICG was recorded. Cells were incubated with culture medium without ICG for 16 h. Release of cellular ICG dye was examined under microscopy.

2.10. RT-PCR, RNA-Seq and ELISA

Total RNA was extracted using Trizol reagent (Sigma-Aldrich) and reversely transcribed using Promega's transcription system according to the manufacturer's instructions. All primers for RT-PCR are listed in Supplementary Table. A total amount of 3 μg RNA were used for RNA-seq. RNA quantification, library preparation, and sequencing were performed at Novogene (Beijing, China) (www.novogene.com).

FVIIII antigen (*FVIII*:Ag) was quantified in the medium supernatants (without serum) using an ELISA kit (Cedarlane) according to the manufacturer's recommendations. Standard curves were constructed using serial dilutions of pooled plasma (Pacific Hemostasis), with correlation coefficient (R2) of at least 0.990 using a 4-parameter logistic curve fit algorithm.

3. Results

3.1. Gene targeting at rDNA locus of human embryonic stem cells

For gene targeting, the rDNA targeting plasmid pHrn-FVIII, which carrys an expression cassette of CMV promoter-driven human B-domain-deleted *FVIII* open reading frame was constructed in our previous

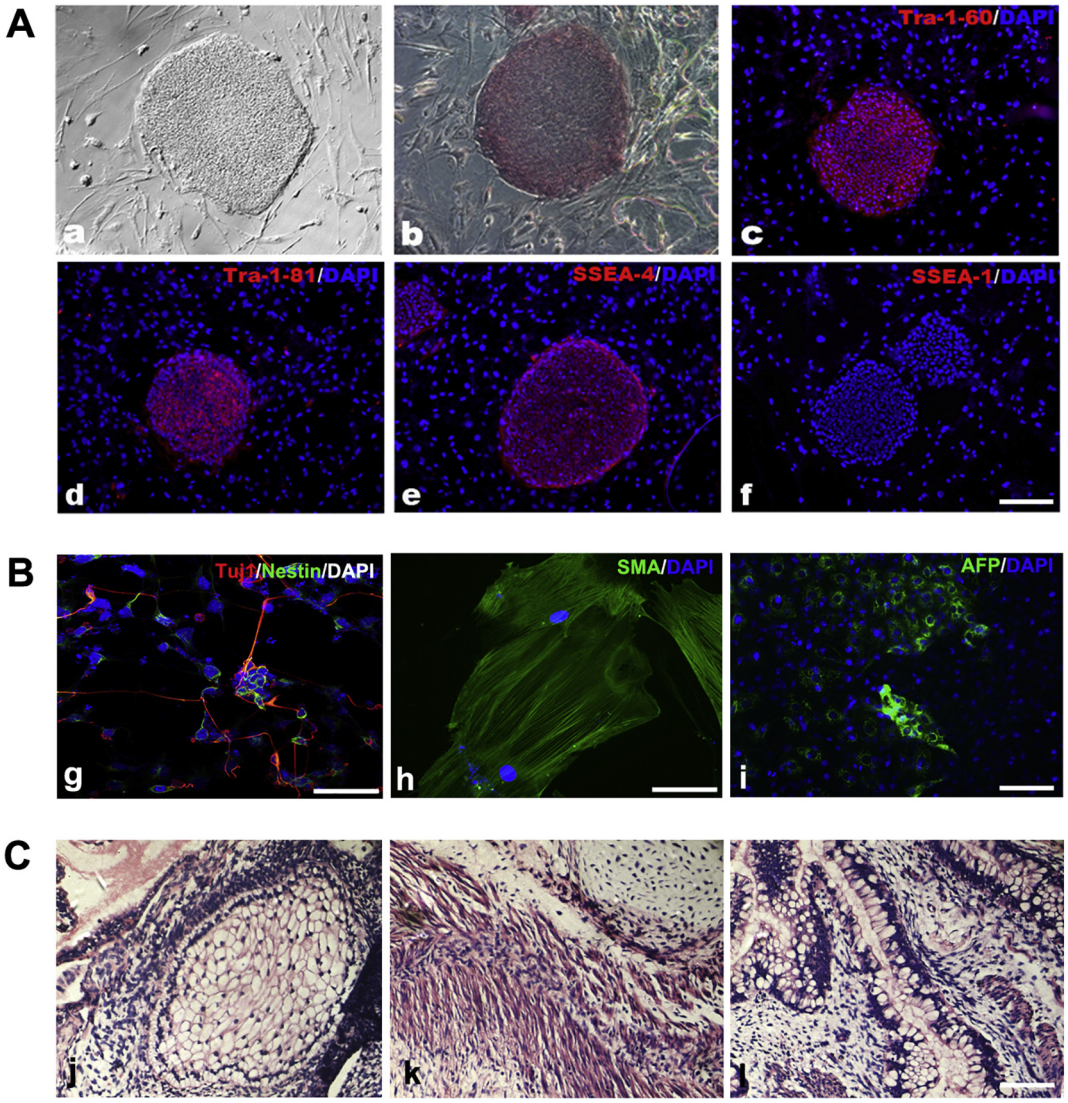

Fig. 2. Characterization of H9-F8 clones. (A) Morphology of H9-F8 clone and expression of specific markers. (a) Phase-contrast image of a H9-F8 clone. (b) Alkaline phosphatase staining of H9-F8. (c–f) Immunofluorescent staining of H9-F8 with Tra-1-60, Tra-1-81, SSEA-4 and SSEA-1 antibodies. Scale bar = 200 μm. (B) *In vitro* differentiation of H9-F8. Immunofluorescent staining exhibited that a portion of differentiated cells were positive for the markers of three germ layers respectively, including ectodermal marker Tuj1 (g), mesodermal marker SMA (h) and endodermal marker AFP (i). Scale bar, g and h = 50 μm, *i* = 200 μm. (C) *In vivo* differentiation from teratoma formed by H9-F8 cells. H&E staining for teratomas tissues displayed derivatives of all three germ layers, including squamous epithelium for ectoderm (j), muscle and cartilage for mesoderm (k), respiratory epithelium for endoderm (l). Scale bar = 100 μm.

studies (Fig. 1A) [8]. The hES H9 cells were electroporated with the linearized targeting construct. Following transfection and G418 selection (Fig. 1B, C), resistant clones were picked and analyzed by PCR for screening of rDNA site-specific integration. Results showed that out of 50 clones, 2 were identified to be positive (Fig. 1D). Sequence analysis of the specific PCR fragments in these clones confirmed the integration of targeting vector into the rDNA locus (Fig. 1E). The targeted-positive clones were further verified to be rDNA-specific integrated by Southern blotting using an external genomic probe (Fig. 1F). A subclone of the targeted clones, designated H9-F8, was used for subsequent experiments.

3.2. Characterization of FVIII targeted hESCs clone

To confirm whether gene targeting at rDNA locus will affect the properties of hESCs, we first measured the alkaline phosphatase activity in H9-F8 using an *in situ* assay. Results revealed that H9-F8 retained alkaline phosphatase activity (Fig. 2A). Expression of stage-specific embryonic antigens TRA-1-60, TRA-1-81, SSEA-4 and SSEA-1, the characteristic feature of primary hESCs, was conformed with immunofluorescent staining (Fig. 2A).

As pluripotent cells, hESCs can differentiate into three germ layers. To confirm that H9-F8 maintains the pluripotency, we performed embryoid body formation and differentiation assays *in vitro*. Expression of endoderm-, mesoderm-, and ectoderm-specific markers in the embryoid body-derived cells were determined to be positive by using immunofluorescent staining with α-fetoprotein (AFP), mesoderm smooth muscle actin (SMA), and beta-III Tubulin (Tuj I), respectively, indicating that rDNA targeted hESCs held the ability to differentiate into three lineages *in vitro* (Fig. 2B).

To further demonstrate the pluripotency of the targeted clone *in vivo*, H9-F8 was evaluated by teratomas formation. Eight weeks after subcutaneous injection into SCID mice, teratomas were dissected and histological analysis was performed. Hematoxylin and eosin staining revealed derivatives of the three layers, including stratified squamous epithelium (ectoderm), cartilage (mesoderm), smooth muscle (mesoderm), and intestine epithelium (endoderm) (Fig. 2C). Thus, the targeted clone maintained the pluripotency *in vivo*.

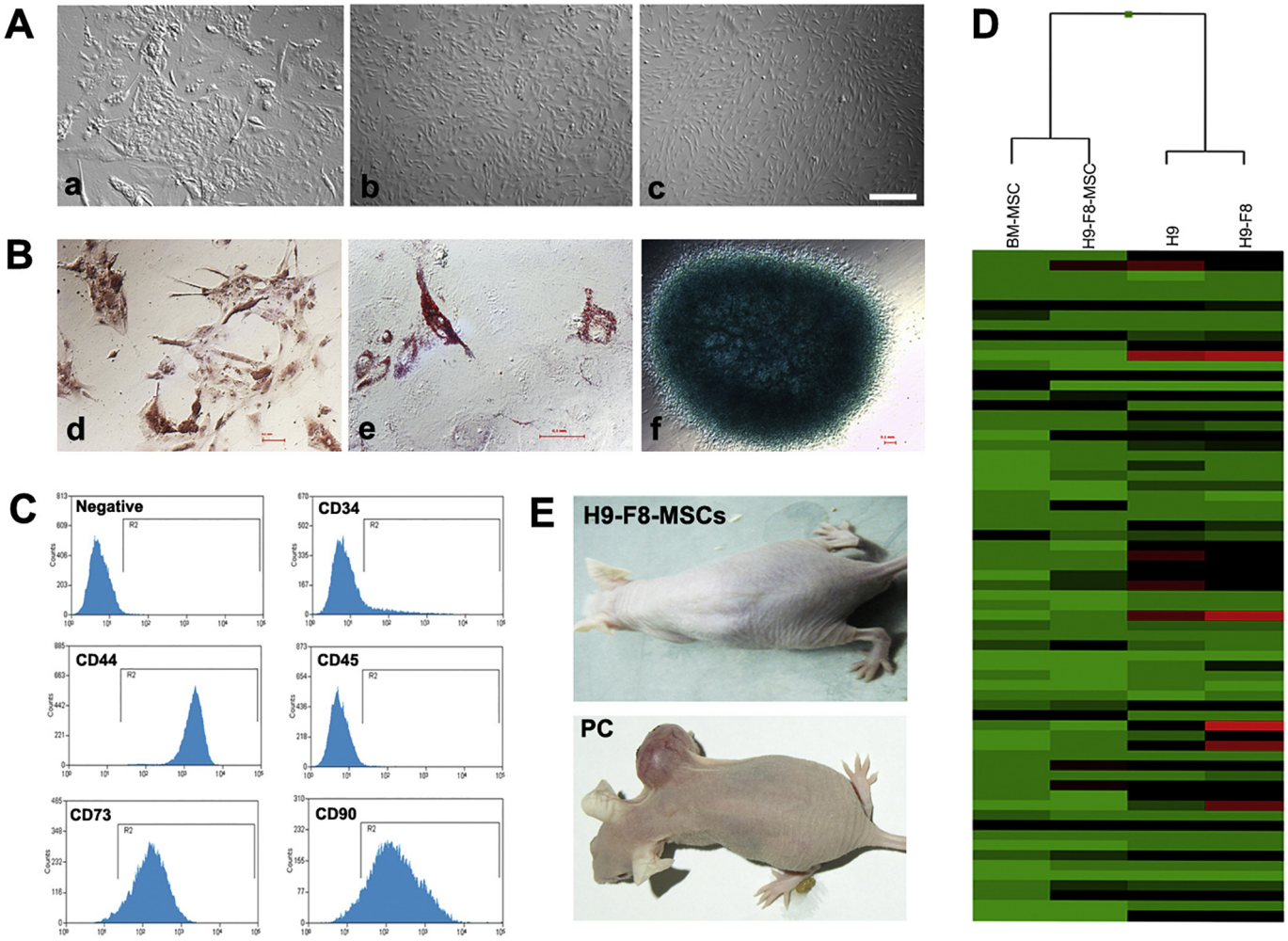

Fig. 3. Differentiation of H9-F8 into MSCs and Characterization. (A) Morphology change of H9-F8-MSCs at different time points. Phase-contrast images show the differentiation of H9-F8 into MSCs on day 5 (a) and 15 (b), as well as the control cell BM-MSCs (c). Scale bar = 200 μm (B) Osteogenic, adipogenic, and chondrogenic multi-lineage differentiated potential of H9-F8-MSCs were detected by staining with alkaline phosphatase (d), oil red O (e) and alcian blue dye (f). Scale bars = 100 μm. (C) Flow cytometry analysis of H9-F8-MSCs to detect surface markers that define human MSCs. (D) Hierarchical clustering analysis of gene expression from BM-MSCs, H9-F8-MSCs, H9 and H9-F8, revealing that H9-F8-MSCs were more hierarchically closely associated with BM-MSCs. (E) Assay for tumor formation with H9-F8-MSCs and Bel7402 as positive control (PC), showing that H9-F8-MSCs would not generate tumor. (For interpretation of the references to colour in this figure legend, the reader is referred to the web version of this article.)

In addition, after extensive passaging, H9-F8 still maintained a normal karyotype with 46, XX (20 passages; Supplementary Fig. 1A). All these results suggested that targeting to the rDNA locus would not affect the main characteristics and differentiation potential of hESCs.

3.3. Differentiation of FVIII targeted hESCs into MSCs

MSCs, as multipotent cells, had been proven to contribute to the functional *FVIII* pool and facilitate transplantation [20, 23]. Here, H9-F8 were trypsinized and cultured in optimized MSC differentiation medium containing epidermal growth factor (EGF) and platelet-derived growth factor-BB (PDGF-BB) for 15 days. After several passages, these cells uniformly displayed a fibroblast-like morphology similar to that of MSCs isolated from bone marrow (BM-MSCs) (Fig. 3A). As expected, the expression of pluripotent transcription factors, such as OCT4, Nanog and SOX2, was generally reduced in H9-F8 derived MSCs (H9-F8-MSCs), indicating transition of pluripotency to multipotency (Supplementary Fig. 2A). We examined the differentiation potential of H9-F8-MSCs *via* histochemical staining and found that induced cells were positive for adipogenesis, osteogenesis and chondrogenesis (Fig. 3B). Analysis of cell surface markers of H9-F8-MSCs by flow cytometry showed expression pattern identical to BM-MSCs, with positivity for CD44, CD73, and CD90, and negativity for CD34 and CD45(Fig. 3C, Supplementary Fig. 2B). Furthermore, gene expression profiles of BM-MSCs, H9-F8-MSCs, H9 and H9-F8 were determined by RNA-Seq and hierarchical clustering analyses. The results showed that H9-F8-MSCs were hierarchically close with BM-MSCs, while H9 and H9-F8 had almost the same gene expression profile (Fig. 3D). Together, these results confirmed that H9-F8 could efficiently differentiate into MSCs.

In consideration of the safety issue, we found that the H9-F8-MSCs could be maintained in continuous culture and keep a normal karyotype for at least 19 passages (Supplementary Fig. 1B). 8 weeks after injection with H9-F8-MSCs and hepatocellular carcinoma cell line Bel7402 (as positive control) into nude mice, respectively, Bel7402 group showed tumor formation, but not H9-F8-MSCs group (Fig. 3E), suggesting a diminished tumorgenic risk of differentiated MSCs.

3.4. Differentiation of FVIII targeted hESCs into hepatocytes and functionality tests

Since several studies have reported that both hESCs and MSCs can differentiate into hepatocytes and synthesized *FVIII* proteins [22, 36], we tried to directly differentiate H9-F8 into functional hepatocytes. Formed EBs were seeded on 5% matrigel in medium and induced by

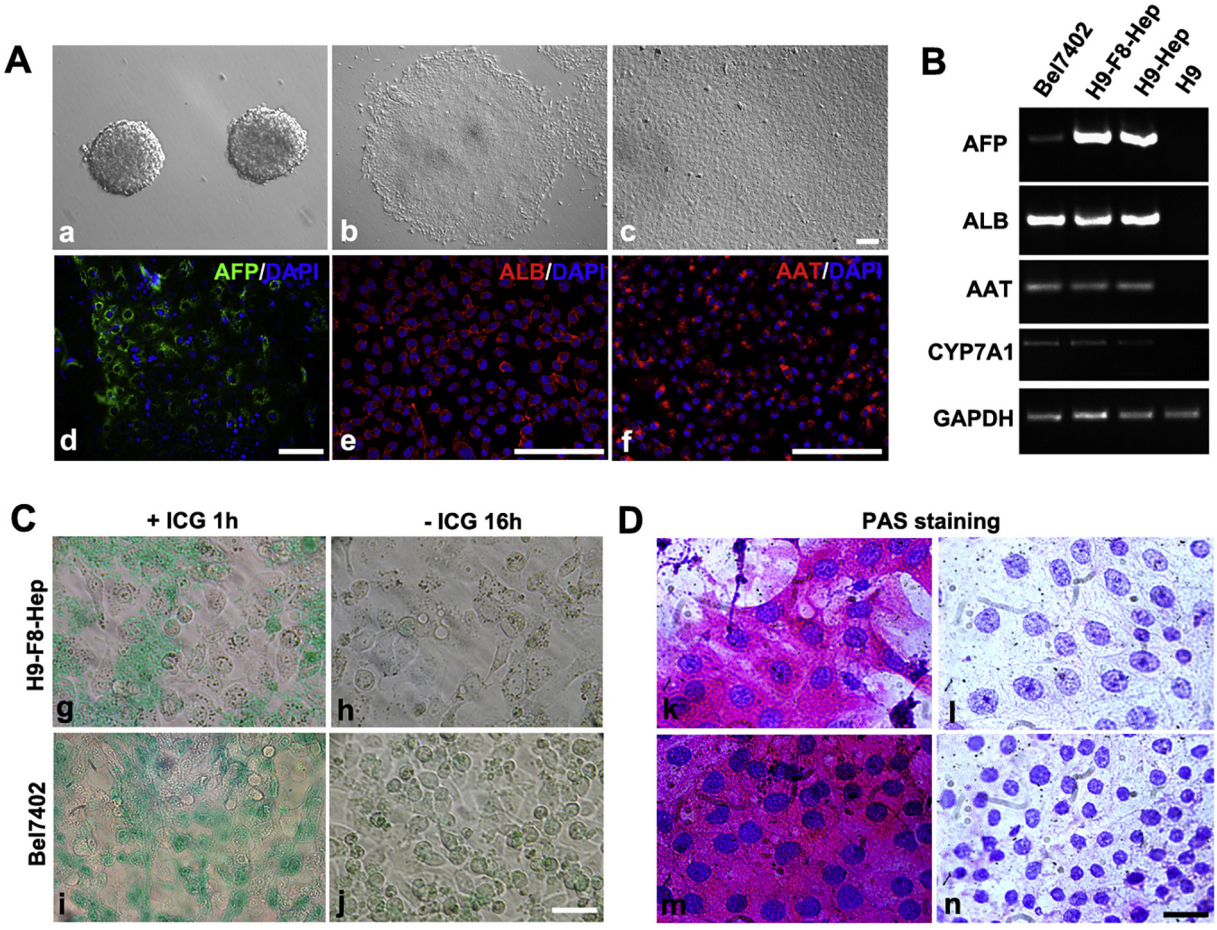

Fig. 4. Direct differentiation of H9-F8 into hepatocytes. (A) Morphology change of H9-F8-Hep during different time and immunofluorescent staining with hepatocyte markers. Phase-contrast images show the H9-F8 formed EBs on day 2 (a) and differentiation into hepatocytes on day 9 (b) and 15 (c). Immunofluorescent staining for H9-F8-Hep with hepatocyte markers, including AFP (d), ALB (e) and AAT (f). Scale bars = 100 μm. (B) RT-PCR analysis of hepatocyte maker genes for H9-F8-Hep, involving AFP, ALB, AAT, CYP7A1. Bel7402 and H9 served as positive and negative controls, respectively. (C) H9-F8-Hep on day 21 were incubated with indocyanine green (ICG) for 1 h (g) and the cellular excretion of ICG was examined at 16 h after the removal of ICG (h). Bel7402 as positive control (i and j). Scale bar = 50 μm. (D) Periodic acid-Schiff's staining for H9-F8-Hep on day 21. Most of differentiated cells displayed pink staining in cytoplasm, suggesting glycogen storage (k), while a small portion of differentiated cells showed no staining (l). Bel7402 as positive control (m) and H9 as negative control (n). Scale bar = 25 μm. (For interpretation of the references to colour in this figure legend, the reader is referred to the web version of this article.)

various factors at different stages. On day 3 of induction, the cells showed a polygonal shape, and the feature became more pronounced by day 9. Most of these cells were epithelioid or fibroblast-like. On day 15, cells were more homogeneous and polygonal in shape with large, round and centered nuclei, like hepatocyte (Fig. 4A). The differentiated cells were confirmed to express specific markers of hepatic lineage cells by RT-PCR, like AFP for hepatic progenitor cells and ALB, AAT, and CYP7A1 for hepatocyte, which were in accordance with positive control Bel7402 (Fig. 4B). Further immunofluorescence stained by anti-AFP, anti-ALB and anti-AAT were located on different clusters of derived cells in the same well, in line with the RT-PCR results (Fig. 4A). Both AFP and ALB expression may indicate that the differentiated cell population contained both hepatic progenitor cells and mature hepatocytes during the induction.

To further evaluate the functionality of derived hepatocyte-like cells, differentiated cells were first performed with the assessment for uptake and release of indocyanine green (ICG), which is a specific functional characteristic of mature hepatocytes. The results demonstrated that a high percentage of ICG-positive cells were visible both in H9-F8-derived hepatocytes on day 21 and positive control Bel7402 after 1 h incubation with ICG (Fig. 4C). In contrast, hESCs did not take any ICG (Supplementary Fig. 3A). Sixteen hours after removal of ICG from the medium, most of ICG were excreted from the cells (Fig. 4C). We also measured the capacity of differentiated cell populations to store glycogen, another physiological function of mature hepatocytes, using the Periodic Acid-Schiff (PAS) staining procedure. We found that a crowd of hepatocyte-like cells on day 21 exhibited PAS-positivity,-supporting differentiation toward hepatocytes (Fig. 4D; Supplementary Fig. 3B). Subsequent tumorgenesis testing for differentiated hepatocytes showed no tumor generation (Supplementary Fig. 3C).

3.5. *FVIII expression in MSCs and hepatocytes derived from FVIII targeted hESCs*

To address whether expression of exogenous B-domain-deleted *FVIII* were obtained in rDNA targeted H9-F8 derived functional MSCs (H9-F8-MSCs) and hepatocytes (H9-F8-Hep), RT-PCR analysis were used to detect the *FVIII* mRNA transcription from these cells. *FVIII* targeted hepatic immortalized cell line (HL7702) which was established in our previous study, was used as positive control [8]. As expected, exogenous *FVIII* mRNA was only detected in rDNA targeted cells, including H9-F8, H9-F8-MSC, H9-F8-Hep and HL7702-F8, but not present in H9, H9 derived cells (H9-MSCs and H9-Hep) and BM-MSCs (Fig. 5A), while endogenous *FVIII* mRNA was present in all cultured cells. These results revealed that the expression cassette of exogenous B-domain-deleted *FVIII* could be ectopically transcribed in rDNA locus.

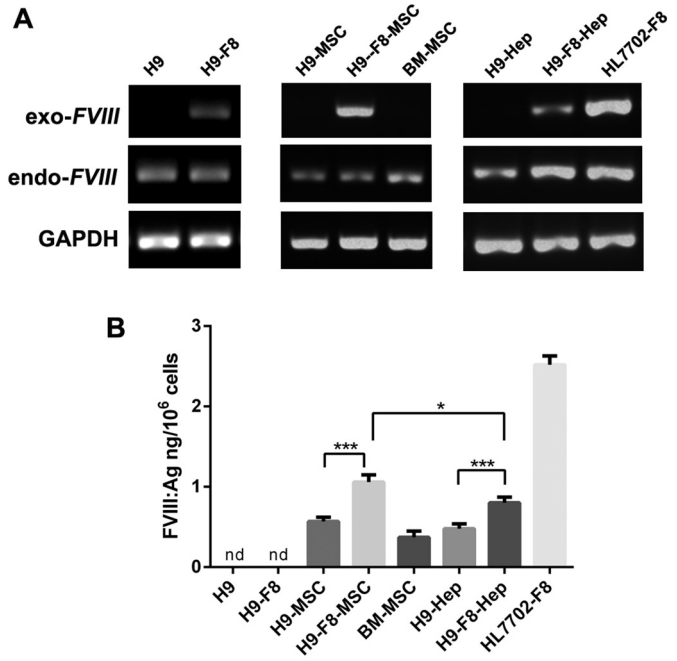

Fig. 5. FVIII expression in H9-F8-MSCs and H9-F8-Hep. (A) RT-PCR analysis of FVIII expression. *Exo-FVIII* represents exogenous B-domain-deleted *FVIII*. *endo-FVIII* represents endogenous wild type *FVIII*. HL7702-F8 was *FVIII* targeted hepatic immortalized cell line, which was established in our previous study, serving as a positive control. (B) ELISA detection for FVIII antigen in medium supernatant from cultured cells. nd, not detected.(Mean ± SEM, $n = 3$ for each group. $^{*}p < .05$, $^{***}p < .001$, One-way ANOVA. Data are representative of two independent replications).

For the secretion of *FVIII* proteins, the medium supernatants collected from all cultured cells were tested by ELISA. The results indicated that despite the transcription of *FVIII* in H9 and H9-F8, secretion of *FVIII* proteins could not be detected in these undifferentiated hESCs (Fig. 5B). In contrast, all other differentiated cells and control cells secreted the *FVIII* proteins at different level. Except for the positive control cells HL7702-F8, H9-F8-MSC showed the highest *FVIII* secretion at the level of 1.06 ± 0.09 ng/10^6 cells, which was significantly higher than H9-MSC and control cells BM-MSC with 0.57 ± 0.05 ng/106 cells and 0.37 ± 0.08 ng/10^6 cells ($p < .01$) respectively (Fig. 5B). H9-F8-Hep secreted the *FVIII* proteins at 0.8 ± 0.07 ng/10^6 cells, which was also significantly higher than H9-Hep with 0.48 ± 0.06 ng/10^6 cells ($p < .01$),but much lower than control cells HL7702-F8 with 2.52 ± 0.11 ng/10^6 cells (Fig. 5B). Compared with untargeted cells, it was reasonable to speculate that the exogenous *FVIII* proteins could be translated and secreted, and thus, contributed to the increase of total *FVIII* proteins in rDNA-specific integrated hESCs derived cells.

4. Discussion

HA is a monogenic disorder and even a slight increase (about 5%) in plasma FVIII activity could ameliorate the bleeding symptom. Hence, HA is considered an attractive model for gene therapy research. Extensive studies have been implemented for hemophilia using different vectors and strategies. Recent years witnessed an encouraging development that viral vector-based gene therapy for hemophilia has proceeded into phase 1/2 clinical trials [1, 3], though a continued caution exists regarding immune response, long-term safety and efficacy [1, 5]. Here, we used a novel non-viral targeting vector pHrn to mediate exogenous FVIII expression cassette integrating into the rDNA locus of hESCs, with the purpose of developing a stem cell-based gene therapy for HA.

The human rDNA locus exhibits high recombination activity during both meiosis and mitosis, indicating that the HR of this area is highly effective [9]. In addition, hundreds of rDNA copies per cell can serve as potential targets for transgenes. Although HR efficiency could be further improved with the use of artificial nuclease, like TALEN and Crispr/Cas9 [37, 38], the potential off-target and cell toxicity are still under assessment [39–41]. In the present study, without the help of any artificial nuclease, we successfully transduced a large DNA fragment of *FVIII* expression cassette into hESCs using eletroporation, and obtained 2 rDNA-specific integration clones out of 50 resistant clones (targeting efficiency at 4%), supporting a high HR efficiency in rDNA region.

Balanced chromosomal translocation involving the rDNA, for example Robertsonian translocation, usually does not show phenotypic effects and can be inherited stably [11]. For this reason, we presumed that transgenes targeted into the rDNA locus would also keep be stable without unexpected effects. Our study provided evidence that the rDNA targeted hESCs clone after dozens of passages still kept their main characteristics, including the expression pattern of specific markers, pluripotent properties for differentiation into three embryonic layers, and normal karyotype. Therefore, rDNA locus would be a safe harbor for transgene and presents great promise in cell-based gene therapy for monogenic diseases.

The choice of target cells capable of producing sufficient and lasting levels of *FVIII* has a major impact on the success of cell-based therapy for HA [2]. hESCs, as pluripotent cells, integrated with *FVIII* expression cassette could represent a long-term source for differentiation into transplantable cells. In this study, we differentiated the *FVIII*-integrated hESCs into functional MSCs and hepatocytes using our optimized protocol. We found either differentiated MSCs or hepatocytes could express related cell markers, display their physiological functionalities and have low risk of tumorgenesis. Particularly, differentiated MSCs could be sufficiently expanded by over 10 passages and purified into a homogeneous population with a homogeneous expression pattern. The differentiated hepatocyte population contained both hepatic progenitor cells and mature hepatocytes in our study, suggesting that extension of induction time may be required to obtain more mature functional hepatocytes. Recent reports revealed that MSCs may express a high level of transcription factors involved in liver development and have the ability to transdifferentiate into mature hepatocytes [36, 42]. Hereby, co-translantation with the differentiated MSCs and hepatocytes may offer reciprocal benefits for *in vivo*.

We detected the *FVIII* expression among the targeted cells. In addition, *FVIII* proteins were present in the supernatant of all differentiated cells. But in undifferentiated targeted hESCs H9-F8, either endogenous or exogenous *FVIII* mRNA or protein was detected. Similar findings were also displayed in mouse ESCs [34]. This may be related to different process of *FVIII* protein modifications in specific cell types, although the exact mechanism is still unclear. Within the differentiated cells, *FVIII* production of the genetic modified MSCs and hepatocytes were significantly higher than that of normal cells, implying that the exogenous *FVIII* proteins have been secreted, thus, increased the total proteins. Between the differentiated MSCs and hepatocytes, we found that regardless of cells derived from genetically modified or normal hESCs, *FVIII* proteins secreted from differentiated MSCs were higher than hepatocytes, even than BM-MSCs. The possible reason for this could be that the differentiated MSC populations were more homogeneous and uniform than that of hepatocytes. With regard to the low level of BM-MSCs, previous study revealed that MSCs isolated from different tissues, such as lung, liver, brain, and bone marrow, had different level of FVIII production. Of all, lung derived MSCs exhibited the highest FVIII activity, while bone marrow generated the lowest level [23].

In summary, we used a nonviral rDNA-targeting vector pHrn to target B-domain-deleted *FVIII* into hESCs. The site-specific integrated hESCs retained the main properties and could be directly differentiated into functional MSCs and hepatocytes, which could stably secret exogenous FVIII protein. These findings have built a foundation for future

animal studies using co-transplantation to facilitate the cell-based therapy for hemophilia A.

5. Conclusions

We have efficiently integrated the B-domain-deleted *FVIII* into the rDNA locus of hESCs and were able to differentiate into MSCs and hepatocytes with stable expression of exogenous FVIII. This hESCs-based rDNA gene targeting strategy would provide a persistent source for producing transplantable donor cells for hemophilia A treatment.

Conflicts of interest

The authors declare that they have no conflict of interest

Funding statement

This work was supported by the National Natural Science Foundation of China (81470299, 31571313 and 81770200) and the National Key Research and Development Program of China (2016YFC0905102).

Appendix A. Supplementary data

Supplementary data to this article can be found online at https://doi.org/10.1016/j.cca.2018.08.007.

References

[1] A.C. Nathwani, A.M. Davidoff, E.G.D. Tuddenham, Advances in gene therapy for hemophilia, Hum. Gene Ther. 28 (11) (2017) 1004–1012.
[2] M.E. Fomin, P.P. Togarrati, M.O. Muench, Progress and challenges in the development of a cell-based therapy for hemophilia A, J. Thromb. Haemost. 12 (12) (2014) 1954–1965.
[3] S. Rangarajan, L. Walsh, W. Lester, D. Perry, B. Madan, M. Laffan, H. Yu, C. Vettermann, G.F. Pierce, W.Y. Wong, K.J. Pasi, AAV5-factor VIII gene transfer in severe hemophilia a, N. Engl. J. Med. 377 (26) (2017) 2519–2530.
[4] L.A. George, Hemophilia gene therapy comes of age, Blood Adv. 1 (26) (2017) 2591–2599.
[5] P. Colella, G. Ronzitti, F. Mingozzi, Emerging issues in AAV-mediated in vivo gene therapy, Mol. Ther. Methods & Clin. Develop. 8 (2018) 87–104.
[6] H. Nakai, E. Montini, S. Fuess, T.A. Storm, M. Grompe, M.A. Kay, AAV serotype 2 vectors preferentially integrate into active genes in mice, Nat. Genet. 34 (3) (2003) 297–302.
[7] X. Liu, Y. Wu, Z. Li, J. Yang, J. Xue, Y. Hu, M. Feng, W. Niu, Q. Yang, M. Lei, J. Xia, L. Wu, D. Liang, Targeting of the human coagulation factor IX gene at rDNA locus of human embryonic stem cells, PLoS One 7 (5) (2012) e37071.
[8] X. Liu, M. Liu, Z. Xue, Q. Pan, L. Wu, Z. Long, K. Xia, D. Liang, J. Xia, Non-viral ex vivo transduction of human hepatocyte cells to express factor VIII using a human ribosomal DNA-targeting vector, J. Thromb. Haemost. 5 (2) (2007) 347–351.
[9] D.M. Stults, M.W. Killen, H.H. Pierce, A.J. Pierce, Genomic architecture and inheritance of human ribosomal RNA gene clusters, Genome Res. 18 (1) (2008) 13–18.
[10] K. Sakai, T. Ohta, S. Minoshima, J. Kudoh, Y. Wang, P.J. de Jong, N. Shimizu, Human ribosomal RNA gene cluster: identification of the proximal end containing a novel tandem repeat sequence, Genomics 26 (3) (1995) 521–526.
[11] P. Steinbach, M. Djalali, I. Hansmann, E. Kattner, M. Meisel-Stosiek, H.D. Probeck, A. Schmidt, M. Wolf, The genetic significance of accessory bisatellited marker chromosomes, Hum. Genet. 65 (2) (1983) 155–164.
[12] J. Yang, X. Liu, J. Yu, L. Sheng, Y. Shi, Z. Li, Y. Hu, J. Xue, L. Wu, Y. Liang, J. Xia, D. Liang, A non-viral vector for potential DMD gene therapy study by targeting a minidystrophin-GFP fusion gene into the hrDNA locus, Acta Biochim. Biophys. Sin. 41 (12) (2009) 1053–1060.
[13] Y. Hu, X. Liu, P. Long, D. Xiao, J. Cun, Z. Li, J. Xue, Y. Wu, S. Luo, L. Wu, D. Liang, Nonviral gene targeting at rDNA locus of human mesenchymal stem cells, Biomed. Res. Int. 2013 (2013) 135189.
[14] N. Yadav, S. Kanjirakkuzhiyil, M. Ramakrishnan, T.K. Das, A. Mukhopadhyay, Factor VIII can be synthesized in hemophilia a mice liver by bone marrow progenitor cell-derived hepatocytes and sinusoidal endothelial cells, Stem Cells Dev. 21 (1) (2012) 110–120.
[15] N. Yadav, S. Kanjirakkuzhiyil, S. Kumar, M. Jain, A. Halder, R. Saxena, A. Mukhopadhyay, The therapeutic effect of bone marrow-derived liver cells in the phenotypic correction of murine hemophilia a, Blood 114 (20) (2009) 4552–4561.
[16] M.E. Fomin, Y. Zhou, A.I. Beyer, J. Publicover, J.L. Baron, M.O. Muench, Production of factor VIII by human liver sinusoidal endothelial cells transplanted in immunodeficient uPA mice, PLoS One 8 (10) (2013) e77255.
[17] E.E. Filali, J.K. Hiralall, H.A. van Veen, D.B. Stolz, J. Seppen, Human liver endothelial cells, but not macrovascular or microvascular endothelial cells, engraft in the mouse liver, Cell Transplant. 22 (10) (2013) 1801–1811.
[18] P. Krause, M. Rave-Frank, H.A. Wolff, H. Becker, H. Christiansen, S. Koenig, Liver sinusoidal endothelial and biliary cell repopulation following irradiation and partial hepatectomy, World J. Gastroenterol. 16 (31) (2010) 3928–3935.
[19] M. Banshodani, T. Onoe, M. Shishida, H. Tahara, S. Hashimoto, Y. Igarashi, Y. Tanaka, H. Ohdan, Adoptive transfer of allogeneic liver sinusoidal endothelial cells specifically inhibits T-cell responses to cognate stimuli, Cell Transplant. 22 (9) (2013) 1695–1708.
[20] M. Fernandez-Garcia, R.M. Yanez, R. Sanchez-Dominguez, M. Hernando-Rodriguez, M. Peces-Barba, G. Herrera, J.E. O'Connor, J.C. Segovia, J.A. Bueren, M.L. Lamana, Mesenchymal stromal cells enhance the engraftment of hematopoietic stem cells in an autologous mouse transplantation model, Stem Cell Res Ther 6 (2015) 165.
[21] Y. Wang, X. Yu, E. Chen, L. Li, Liver-derived human mesenchymal stem cells: a novel therapeutic source for liver diseases, Stem Cell Res Ther 7 (1) (2016) 71.
[22] J. Cao, C.Z. Shang, L.H. Lu, D.C. Qiu, M. Ren, Y.J. Chen, J. Min, Differentiation of embryonic stem cells into hepatocytes that coexpress coagulation factors VIII and IX, Acta Pharmacol. Sin. 31 (11) (2010) 1478–1486.
[23] C. Sanada, C.J. Kuo, E.J. Colletti, M. Soland, S. Mokhtari, M.A. Knovich, J. Owen, E.D. Zanjani, C.D. Porada, G. Almeida-Porada, Mesenchymal stem cells contribute to endogenous FVIII:c production, J. Cell. Physiol. 228 (5) (2013) 1010–1016.
[24] T. Ohmori, H. Mizukami, K. Ozawa, Y. Sakata, S. Nishimura, New approaches to gene and cell therapy for hemophilia, J. Thromb. Haemost. 13 (Suppl. 1) (2015) S133–S142.
[25] C.D. Porada, C. Sanada, C.J. Kuo, E. Colletti, W. Mandeville, J. Hasenau, E.D. Zanjani, R. Moot, C. Doering, H.T. Spencer, G. Almeida-Porada, Phenotypic correction of hemophilia A in sheep by postnatal intraperitoneal transplantation of FVIII-expressing MSC, Exp. Hematol. 39 (12) (2011) 1124–1135 (e4).
[26] Q. Wang, X. Gong, Z. Gong, X. Ren, Z. Ren, S. Huang, Y. Zeng, The mesenchymal stem cells derived from transgenic mice carrying human coagulation factor VIII can correct phenotype in hemophilia A mice, Journal of genetics and genomics = Yi chuan xue bao 40 (12) (2013) 617–628.
[27] M.M. Bonab, K. Alimoghaddam, F. Talebian, S.H. Ghaffari, A. Ghavamzadeh, B. Nikbin, Aging of mesenchymal stem cell in vitro, BMC Cell Biol. 7 (2006) 14.
[28] R. Guo, X. Xu, Y. Lu, X. Xie, Physiological oxygen tension reduces hepatocyte dedifferentiation in in vitro culture, Sci. Rep. 7 (1) (2017) 5923.
[29] A. Choo, S.K. Lim, Derivation of mesenchymal stem cells from human embryonic stem cells, Methods Mol. Biol. 690 (2011) 175–182.
[30] X. Ma, Y. Duan, B. Tschudy-Seney, G. Roll, I.S. Behbahan, T.P. Ahuja, V. Tolstikov, C. Wang, J. McGee, S. Khoobyari, J.A. Nolta, H. Willenbring, M.A. Zern, Highly efficient differentiation of functional hepatocytes from human induced pluripotent stem cells, Stem Cells Transl. Med. 2 (6) (2013) 409–419.
[31] K. Takayama, M. Inamura, K. Kawabata, K. Katayama, M. Higuchi, K. Tashiro, A. Nonaka, F. Sakurai, T. Hayakawa, M.K. Furue, H. Mizuguchi, Efficient generation of functional hepatocytes from human embryonic stem cells and induced pluripotent stem cells by HNF4alpha transduction, Mol. Ther. 20 (1) (2012) 127–137.
[32] V. Volarevic, B.S. Markovic, M. Gazdic, A. Volarevic, N. Jovicic, N. Arsenijevic, L. Armstrong, V. Djonov, M. Lako, M. Stojkovic, Ethical and safety issues of stem cell-based therapy, Int. J. Med. Sci. 15 (1) (2018) 36–45.
[33] W.K. Song, K.M. Park, H.J. Kim, J.H. Lee, J. Choi, S.Y. Chong, S.H. Shim, L.V. Del Priore, R. Lanza, Treatment of macular degeneration using embryonic stem cell-derived retinal pigment epithelium: preliminary results in Asian patients, Stem cell reports 4 (5) (2015) 860–872.
[34] S. Kasuda, A. Kubo, Y. Sakurai, S. Irion, K. Ohashi, K. Tatsumi, Y. Nakajima, Y. Saito, K. Hatake, S.W. Pipe, M. Shima, A. Yoshioka, Establishment of embryonic stem cells secreting human factor VIII for cell-based treatment of hemophilia a, J. Thromb. Haemost. 6 (8) (2008) 1352–1359.
[35] S. Kasuda, K. Tatsumi, Y. Sakurai, M. Shima, K. Hatake, Therapeutic approaches for treating hemophilia a using embryonic stem cells, Hematology/oncology and stem cell therapy 9 (2) (2016) 64–70.
[36] D.K. Bishi, S. Mathapati, J.R. Venugopal, S. Guhathakurta, K.M. Cherian, S. Ramakrishna, R.S. Verma, Trans-differentiation of human mesenchymal stem cells generates functional hepatospheres on poly(L-lactic acid)-co-poly(ε-caprolactone)/collagen nanofibrous scaffolds, J. Mater. Chem. B 1 (2013) 3972–3984.
[37] K. Takayama, K. Igai, Y. Hagihara, R. Hashimoto, M. Hanawa, T. Sakuma, M. Tachibana, F. Sakurai, T. Yamamoto, H. Mizuguchi, Highly efficient biallelic genome editing of human ES/iPS cells using a CRISPR/Cas9 or TALEN system, Nucleic Acids Res. 45 (9) (2017) 5198–5207.
[38] Y. Zhang, H. Huang, B. Zhang, S. Lin, TALEN- and CRISPR-enhanced DNA homologous recombination for gene editing in zebrafish, Methods Cell Biol. 135 (2016) 107–120.
[39] T. Koo, J. Lee, J.S. Kim, Measuring and reducing off-target activities of programmable nucleases including CRISPR-Cas9, Mol. Cell 38 (6) (2015) 475–481.
[40] T. Lancet, Editing the human genome: balancing safety and regulation, Lancet 391 (10119) (2018) 402.
[41] J. Corrigan-Curay, M. O'Reilly, D.B. Kohn, P.M. Cannon, G. Bao, F.D. Bushman, D. Carroll, T. Cathomen, J.K. Joung, D. Roth, M. Sadelain, A.M. Scharenberg, C. von Kalle, F. Zhang, R. Jambou, E. Rosenthal, M. Hassani, A. Singh, M.H. Porteus, Genome editing technologies: defining a path to clinic, Mol. Ther. 23 (5) (2015) 796–806.
[42] T. Talaei-Khozani, M. Borhani-Haghighi, M. Ayatollahi, Z. Vojdani, An in vitro model for hepatocyte-like cell differentiation from Wharton's jelly derived-mesenchymal stem cells by cell-base aggregates, Gastroenterology and hepatology from bed to bench 8 (3) (2015) 188–199.